Narrow Bandpass Frequency Selective Surface With High Level of Angular Stability at *Ka*-Band

Hsi-Hsir Chou and Guan-Jhou Ke

***Abstract*— In this letter, a novel design of a narrow bandpass frequency selective surface (FSS) based on the utilization of the coupled method, which resonates at *Ka*-band frequencies between 29 and 30.3 GHz, is proposed and experimentally evaluated. A high selectivity was achieved, by coupling two metallic layers, which were based on the structure of a cross aperture and a rectangle grid patch, respectively. The simple symmetric patterns used in the proposed work have also made the FSS independent of polarization properties. Moreover, a high angular stability was also achieved since for electromagnetic (EM) wave incident at degrees from 0° to 75°, the frequency deviations were only 0.1% and 0.4% for TE and TM polarizations, respectively. For performance evaluation, an experimental FSS prototype was fabricated by a double-sided printed circuit board (PCB), which was composed of 50 × 50 unit cells in a dimension of 18 cm × 18 cm. A Keysight N5227A PNA and two-horn antennas in a chamber were setup to measure the performance. The experimental measurement results have shown a good agreement with the numerical simulations.**

***Index Terms*— Angular stability, bandpass filter, frequency selective surface (FSS), polarization insensitivity.**

I. Introduction

THE frequency selective surface (FSS) has been investigated for decades. Based on the array of periodic structure, the characteristics of frequency selection can be offered. Until now, it has also attracted many researchers to the development of FSS technologies, since it has many applications in microwave and optics, such as reflective antennas, radome, and spatial filter [1], [2]. In these applications, the characteristics of narrow bandpass are normally required.

In order to improve the performance of an FSS, several approaches have been proposed to achieve a narrower bandwidth as well as to improve the quality factor (Q factor), but each has both advantages and disadvantages. Although a narrower bandwidth can be achieved through the method of cascaded FSSs [3], [4], the bulky size and high cost seem not widely accepted. The FSS based on 3-D configuration [5]–[7] was also proposed. A high-frequency selectivity can be achieved due to the characteristic of this complex structure, which can limit the propagation path of electromagnetic (EM) wave. However, it is still a challenge to realize such complex 3-D structure.

Manuscript received September 8, 2020; revised November 12, 2020 and December 31, 2020; accepted January 18, 2021. Date of publication February 5, 2021; date of current version April 8, 2021. This work was supported in part by the National Chung-Shan Institute of Science and Technology, Taiwan under Grant XD909025P400-CS and in part by the Ministry of Science and Technology (MOST), Taiwan under Grant MOST 109-2637-E-011-001. *(Corresponding author: Hsi-Hsir Chou.)*

The authors are with the Department of Electronic and Computer Engineering, National Taiwan University of Science and Technology, Taipei 106, Taiwan (e-mail: hsi-hsir.chou@trinity.cantab.net; M10802310@mail.ntust.edu.tw).

Color versions of one or more figures in this letter are available at https://doi.org/10.1109/LMWC.2021.3054016.

Digital Object Identifier 10.1109/LMWC.2021.3054016

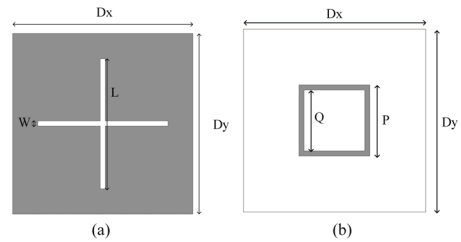

Fig. 1. Geometry of unit cell (a) cross aperture on top and (b) rectangle grid patch on bottom metallic layer.

In this research, a novel design of a narrow bandpass FSS based on the utilization of the coupled method [8], [9], which resonates at *Ka*-band frequencies between 29 and 30.3 GHz, is reported and evaluated experimentally. Based on the utilization of the coupled method and equivalent circuit (EC) model [8], [9], the selectivity, planar structure, and thickness of the proposed FSS were realized and analyzed. A high selectivity was achieved in the proposed work, by coupling the structure of a cross aperture and a rectangle grid patch, respectively. Moreover, polarization insensitivity is achieved due to the symmetric patterns used in the proposed work. Although the FSS design with a high angular stability for EM wave incident at a degree of up to 75° was demonstrated previously, a frequency deviation of 2.2% for TM wave resulted [10]. However, in the proposed work which was based on symmetric structures, for EM wave incident at degrees from 0° to 75°, the frequency deviations can be reduced to 0.1% and 0.4% for TE and TM polarizations, respectively. In comparison with the FSS designs that were presented previously [5], [10], the proposed work offers a better performance in terms of angular stability and polarization-insensitive property.

II. Geometry Design Of FSS Unit Cell

The design of the proposed FSS was based on a periodic unit structure, in which the geometry of each unit cell is shown in Fig. 1. Since in the design of a bandpass filter, the bandwidth can be narrowed by cascading a band-stop filter, a narrow bandwidth in the proposed work was achieved by cascading a bandpass cross aperture and a band-stop rectangle grid patch. Therefore, the unit cell for the proposed FSS is composed of three layers where a dielectric substrate is configured between two metallic layers (top and bottom layers of the unit cell). As illustrated in Fig. 1, the top layer was

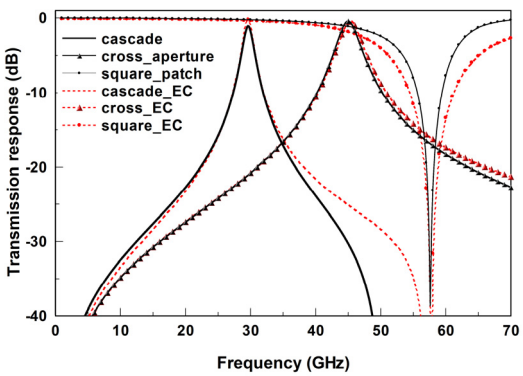

Fig. 2. Effect of single layer and cascade of each other in full-wave simulation and EC model.

designed based on a cross-aperture structure and the bottom layer was designed through the pattern of a rectangle grid patch. The black region represents the metallic structure which was made of copper foil, and the white region illustrates the part of the hollowed out. The metallic patterns were etched on a double-sided printed circuit board (PCB) (RO3003; Rogers Corporation [11]) with a thickness of 0.13 mm. The copper foil has a thickness of 0.035 mm, the relative dielectric constant of substrate is 3, and the loss tangent is 0.001.

For the design of a single-layer filter, the cross aperture (L) and the rectangle grid patch (P) can be calculated in light of the approach provided from the literature [12]. Moreover, it was also known from the literature [13] that the smaller the size of the unit cell (relative to wavelength), the better the angular stability. Therefore, despite the theoretical calculation, a straightforward way to determine the D_x and D_y was through optimization procedures in Ansoft high frequency structure simulator (HFSS) simulations [14]. A high angular stability was also achieved by cascading these geometries in a structure with 0.013 λ in thickness, which has the best coupling effect. However, if the thickness is less than 0.01 λ, a ripple occurs due to oblique incidence. Besides, the coupling effect will also be reduced if the thickness is larger than 0.03 λ. Moreover, the main parameter "L" in cross aperture was used to determine the center frequency and a longer L will result in a lower center frequency. The L, P, and Q has a ratio of 13:7:6, and the optimization results are generated from HFSS [14]. By cascading a bandpass cross aperture and a band-stop rectangle grid patch, an integrated resonating frequency of 29.6 GHz as illustrated in Fig. 2 was formed as well as angular stability improved. From the analysis of the simulation results, the bandpass and band-stop filters were resonated at 46 and 58 GHz, respectively. The EC model that was used to analyze the proposed work is shown in Fig. 3, where the center frequency has been decreased to 29.6 GHz by the capacitance (C_m) between the two layers and it can also be further verified by

$$f_p \approx \frac{1}{2\pi \times \sqrt{L_1 \times (C_1 + C_m)}}. \tag{1}$$

The final parameters of the unit cell marked in Fig. 1 generated from HFSS optimal procedure [14] are as follows: $D_x = D_y = 3.6$ mm, $W = 0.1$ mm, $L = 2.6$ mm, $Q = 1.2$ mm, and $P = 1.4$ mm.

III. Performance of Numerical Simulations

In the numerical simulation of the proposed FSS through Ansoft HFSS software [14], the transmission properties of the electromagnetic field through a periodic element can be simulated via setting the excitation source (floquet port), the master, and the slave boundary conditions in HFSS software. The transmission properties in terms of S-parameter for both TE and TM polarizations are shown in Fig. 4. It is obvious that the proposed FSS design has the property of polarization insensitivity.

The simulation results of the proposed FSS for both TE and TM polarizations with different incident angle are shown in Fig. 5. For the incident angle ranging from 0° to 75°,

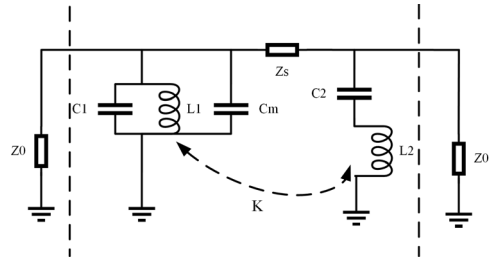

Fig. 3. Equivalent circuit model of the FSS ($C_1 = 0.22$ pF, $C_2 = 0.005$ pF, $L_1 = 0.057$ nH, $L_2 = 1.52$ nH, $C_m = 0.28$ pF, $K = 0.4$, $Z_S = 217.66\ \Omega$, and $Z_0 = 377\ \Omega$).

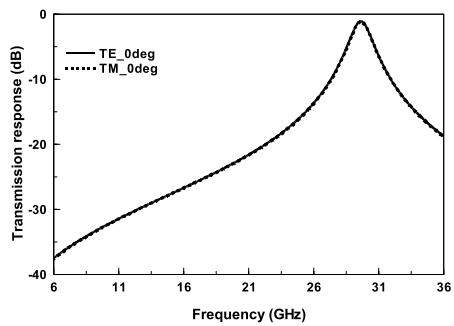

Fig. 4. Comparison of TE and TM polarization at normal incident angle.

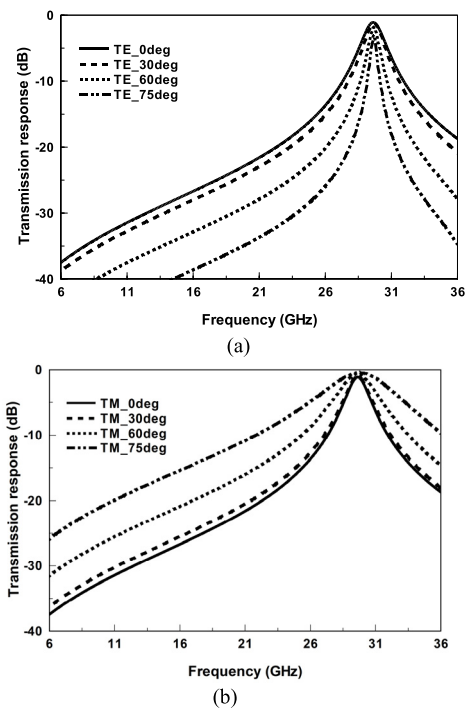

Fig. 5. Transmission response of (a) TE and (b) TM modes under various incident angles.

TABLE I
COMPARE WITH OTHER RELATED FSS DESIGN

Paper	Unit cell size	3dB Bandwidth, f0	Transmission pole	Frequency deviation for TE(%)	Frequency deviation for TM(%)
[15]	7.0mm*7.0mm	18.8%, 2.2GHz	1	1.39(60°)	1.92(60°)
[16]	4.5mm*4.5mm	13.4%, 33.5 GHz	2	N/A (60°)	N/A (60°)
[10]	3.2mm*3.2mm	21.0%, 7.92 GHz	1	N/A (60°, 75°)	0.5 (60°), 2.02(75°)
[17]	6.0mm*6.0mm	13.3%, 15 GHz	2	N/A (60°)	N/A (60°)
[18]	6.0mm*6.0mm	10.0%, 3.8 GHz	2	2(40°), 2.6(60°)	1.8(40°), 2.6(60°)
[19]	4.5mm*4.5mm	20.0%, 10 GHz	2	7(60°)	10(60°)
[20]	3.0mm*3.0mm	5.0%, 21 GHz	2	2.5(40°)	2.3(40°)
This work	3.6mm*3.6mm	4.4%, 29.6 GHz	1	0.03(60°), 0.1(75°)	0.03(60°), 0.4(75°)

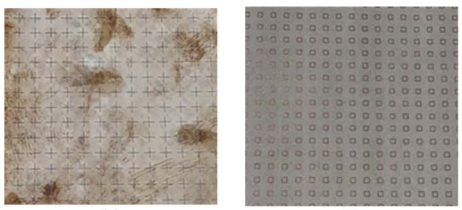

Fig. 6. (a) Top and (b) bottom pattern of fabricated FSS.

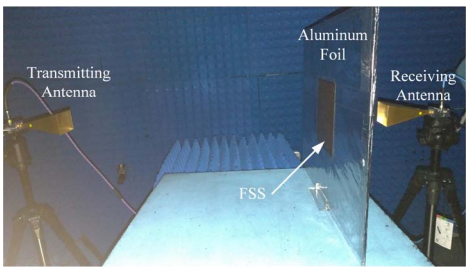

Fig. 7. Measurement setup.

the transmission property for TE polarization as illustrated in Fig. 5 shows that the maximum frequency deviation is only 0.1%, and the TM polarization is 0.4%. A comparison of the proposed FSS design with the state of the art that emphasized on angular stability [10], [15]–[20] was also made and is shown in Table I. It is clear that the proposed FSS design has a better angular stability, in particular the frequency deviations are only 0.03% and 0.4% for the incident angle of 60° and 75°, respectively, which is better than all the cases from previous research [10], [15]–[20].

IV. FABRICATION AND EXPERIMENTAL MEASUREMENTS

In order to evaluate the simulation performance of the proposed FSS, an experimental FSS prototype was fabricated by a double-sided PCB (RO3003; Rogers Corporation [11]) as illustrated in Fig. 6, which was composed of 50 × 50 unit cells in a dimension of 18 cm × 18 cm. A Keysight N5227A PNA and two-horn antennas in a chamber were setup to measure the performance of the proposed FSS.

During the measurements, the fabricated FSS was fixed on a holder made of acrylic in order to measure its angular stability. The setup of the measurements is illustrated in Fig.7, where the distance between two-horn antennas is about 0.8 m. The fabricated FSS prototype was embedded into a rectangle aluminum foil in order to reduce the effect of diffractions. This is an efficient approach used to increase the reliability of measurement, which has been proved in literatures, i.e., [19]. The simulation and experimental results are compared as illustrated in Fig. 8, where the original system loss has been

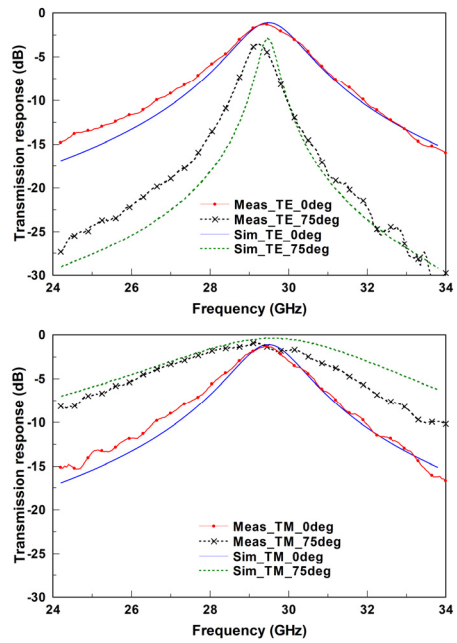

Fig. 8. Comparisons of simulation and measurement results.

deducted in the measurement results. The insertion loss of the fabricated FSS is about 1.25 and 3.21 dB for the incident wave with an incident angle of 0° and 75°, respectively. The 3-dB bandwidth is in the range of 28.75–30.15 GHz, about 4.76% of the center frequency. Maximum frequency deviation is 0.68% for TE and TM mode for incident angles from 0° to 75°. From these comparisons, although the results are not exactly matched due to some tolerances of fabrication, it is obvious that the measurement results have a good agreement with numerical simulations.

V. CONCLUSION

In this letter, a novel design of a narrow bandpass FSS resonating at *Ka*-band frequencies with a 3-dB bandwidth close to 4.4% is reported. The proposed FSS with a polarization insensitivity and a high angular stability was also achieved since for the EM wave incident at degrees from 0° to 75°, the frequency deviations were only 0.1% and 0.4% for TE and TM polarizations, respectively. Besides, the proposed FSS design was based on a simple structure with a thickness of 0.2 mm. In particular, the results from the measurements have shown a good agreement with simulations. The reported work will offer an alternative solution for new FSS design which emphasizes on angular stability and polarization-insensitive property.

REFERENCES

[1] R. Dickie, R. Cahill, V. Fusco, H. S. Gamble, and N. Mitchell, "THz frequency selective surface filters for Earth observation remote sensing instruments," *IEEE Trans. THz Sci. Technol.*, vol. 1, no. 2, pp. 450–461, Nov. 2011.

[2] R. Mittra, C. H. Chan, and T. Cwik, "Techniques for analyzing frequency selective surfaces—A review," *Proc. IEEE*, vol. 76, no. 12, pp. 1593–1615, Dec. 1988.

[3] M. A. Al-Joumayly and N. Behdad, "A generalized method for synthesizing low-profile, band-pass frequency selective surfaces with non-resonant constituting elements," *IEEE Trans. Antennas Propag.*, vol. 58, no. 12, pp. 4033–4041, Dec. 2010.

[4] K. Payne, K. Xu, and J. H. Choi, "Generalized synthesized technique for the design of thickness customizable high-order bandpass frequency-selective surface," *IEEE Trans. Microw. Theory Techn.*, vol. 66, no. 11, pp. 4783–4793, Nov. 2018.

[5] T. Deng, Y. Yu, Z. Shen, and Z. N. Chen, "Design of 3-D multilayer ferrite-loaded frequency-selective rasorbers with wide absorption bands," *IEEE Trans. Microw. Theory Techn.*, vol. 67, no. 1, pp. 108–117, Jan. 2019.

[6] J. Zhu, W. Tang, C. Wang, C. Huang, and Y. Shi, "Dual-polarized bandpass frequency-selective surface with quasi-elliptic response based on square coaxial waveguide," *IEEE Trans. Antennas Propag.*, vol. 66, no. 3, pp. 1331–1339, Mar. 2018.

[7] J. Zhu, Z. Hao, C. Wang, Z. Yu, C. Huang, and W. Tang, "Dual-band 3-D frequency selective surface with multiple transmission zeros," *IEEE Antennas Wireless Propag. Lett.*, vol. 18, no. 4, pp. 596–600, Apr. 2019.

[8] D. Wang, W. Che, Y. Chang, K.-S. Chin, and Y. L. Chow, "A low-profile frequency selective surface with controllable triband characteristics," *IEEE Antennas Wireless Propag. Lett.*, vol. 12, pp. 468–471, 2013.

[9] D. S. Wang, P. Zhao, and C. H. Chan, "Design and analysis of a high-selectivity frequency-selective surface at 60 GHz," *IEEE Trans. Microw. Theory Techn.*, vol. 64, no. 6, pp. 1694–1703, Jun. 2016.

[10] Z. Zhao, J. Li, H. Shi, X. Chen, and A. Zhang, "A low-profile angle-insensitive bandpass frequency-selective surface based on vias," *IEEE Microw. Wireless Compon. Lett.*, vol. 28, no. 3, pp. 200–202, Mar. 2018.

[11] *RO3000 Series Circuit Materials RO3003, RO3006, RO3010 and RO3035 High Frequency Laminates*, Rogers Corporation, Chandler, AZ, USA, 2019.

[12] B. A. Munk, *Frequency Selective Surfaces: Theory and Design*. New York, NY, USA: Wiley, 2000.

[13] K. Sarabandi and N. Behdad, "A frequency selective surface with miniaturized elements," *IEEE Trans. Antennas Propag.*, vol. 55, no. 5, pp. 1239–1245, May 2007.

[14] Ansys Hfss. *High Frequency Electromagnetic Field Simulation Software*. Accessed: May 22, 2020. [Online]. Available: https://www.ansys.com/zh-tw/products/electronics/ansys-hfss

[15] H. Li, C. Yang, Q. Cao, and Y. Wang, "An ultrathin bandpass frequency selective surface with miniaturized element," *IEEE Antennas Wireless Propag. Lett.*, vol. 16, pp. 341–344, 2017.

[16] W. Wu, X. Liu, K. Cui, Y. Ma, and Y. Yuan, "An ultrathin and polarization-insensitive frequency selective surface at Ka-band," *IEEE Antennas Wireless Propag. Lett.*, vol. 17, no. 1, pp. 74–77, Jan. 2018.

[17] N. Liu, X. Sheng, C. Zhang, and D. Guo, "Design of frequency selective surface structure with high angular stability for radome application," *IEEE Antennas Wireless Propag. Lett.*, vol. 17, no. 1, pp. 138–141, Jan. 2018.

[18] M. Hussein, J. Zhou, Y. Huang, and B. Al-Juboori, "A low-profile miniaturized second-order bandpass frequency selective surface," *IEEE Antennas Wireless Propag. Lett.*, vol. 16, pp. 2791–2794, 2017.

[19] M. Al-Joumayly and N. Behdad, "A new technique for design of low-profile, second-order, bandpass frequency selective surfaces," *IEEE Trans. Antennas Propag.*, vol. 57, no. 2, pp. 452–459, Feb. 2009.

[20] S. M. A. Momeni Hasan Abadi and N. Behdad, "Inductively-coupled miniaturized-element frequency selective surfaces with narrowband, high-order bandpass responses," *IEEE Trans. Antennas Propag.*, vol. 63, no. 11, pp. 4766–4774, Nov. 2015.